EXTENDED SHORT WAVE INFRARED TECHNOLOGICAL DEVELOPMENTS AT LYNRED

Nicolas Péré-Laperne[a], Jerôme Fantini[a], Laurent Espuno[a], Jocelyn Berthoz[a], Magalie Maillard[a], Amandine Badina[a], Michel Vuillermet[a]

[(a)] LYNRED, Actipole - CS 10021, 364 route de Valence, 38113 Veurey-Voroize, France

KEYWORDS: eSWIR, HgCdTe, IDDCA, Focal Plane Array

ABSTRACT:

The short wave infrared (SWIR) spectral band is an emerging domain thanks to its large potential. In this spectral region, new opportunities can be found in several fields of applications such as defense and security (night vision, active imaging), space (earth observation), transport (automotive safety), or industry (nondestructive process control, food and plastic sorting). The main technology used for SWIR imaging is based on lattice-matched InGaAs/InP heterostructures. Nevertheless, it is limited in spectral range. For many defense and industrial applications, extended SWIR (eSWIR) would be a significant gain compared to standard SWIR.

At LYNRED, eSWIR is getting much interest for ground applications. This band has been studied, developed and processed for decades for space applications using HgCdTe legacy technology. This material associates high performance with good stability and reliability. Furthermore, the large wafer format and a relatively simple process flow make this technology compatible with a high production yield and capacity. Capitalizing on this experience, LYNRED is developing a focal plane array using this technology for high performance and high speed ground-based applications. In order to deliver the first prototypes, this focal plane array is integrated in an Integrated Detector Dewar Cryocooler Assembly to operate at 190K using the so-called 'plug up platform' already developed for high operating temperature applications in Mid-Wave Infrared range.

1. INTRODUCTION

The short wave infrared (SWIR) spectral band is an emerging domain thanks to its large potential. Close to VISible/Near Infrared wavelengths, SWIR images interpretation is relatively straightforward for the users. In this spectral region, new opportunities can be found in several fields of applications such as defense and security (night vision, active imaging), transport (automotive safety), or industry (nondestructive process control, food and plastic sorting).
For instance, in plastic and textile recycling, it has the potential to improve automated sorting systems by distinguishing materials based on their unique absorption features, leading to more efficient recycling processes. Extended SWIR also has the potential to enhance crop health monitoring by detecting water stress and diseases signatures more efficiently than standard visible or SWIR sensors. Other applications include imaging, spectroscopy, remote sensing, chemical process monitoring, astronomical observation and remote detection of minerals [1]. These examples highlight the broad potential of extended SWIR detectors to enhance efficiency, sustainability and performance across multiple industries.

Although mature, the lattice-matched InGaAs on InP technology cannot address one part of the SWIR spectrum: the so-called eSWIR (extended-SWIR), which extends the SWIR band up to a cutoff wavelength of 2.5µm. This spectral region, from 0.8µm to 2.5µm, opens many opportunities for new applications, as it can provide enhanced material differentiation compared to standard SWIR detectors.

In order to extend the cutoff wavelength, different technologies have been studied. The two commercial technologies are the strained InGaAs and the HgCdTe with the appropriate cutoff wavelength. The strained InGaAs material is still using InP substrate and the cutoff wavelength is defined thanks to the In/Ga ratio. This material is strained with a significant lattice mismatch between the absorber layer and the substrate. This mismatch is leading to a significant increase in dark current compared to the lattice match InGaAs. At 300K, the dark current is in the range of 10^{-2}A/cm2. This result leads to a degraded signal to noise ratio or a lower operating temperature. On the other hand, the second technology mentioned above is based on HgCdTe absorbing material. The best performances are reported using a P/N junction extrinsically doped [2]. The latter material benefits from its ability to adjust the cutoff wavelength by defining the Hg/Cd ratio. The performance in terms of dark current is as low as 10^{-4}A/cm^2 at room temperature with a high QE in the range of 80%.

At LYNRED, the eSWIR technology is mainly developed for space applications [3]. In this frame,

high reliability focal plane arrays were delivered in the past. The technology of these detectors is based on the legacy n/p HgCdTe photodiode array using a Hg vacancy doped absorbing material.

In this paper, the eSWIR high speed HgCdTe demonstrator is deeply described. Each part of the focal plane array (FPA) is presented in a section. First, the detection array is illustrated with the n/p junction using a Hg vacancies doped absorbing material. Second, the Read-Out Integrated Circuit (ROIC) is introduced with the associated figures of merit. In a third part, the Focal Plane Array (FPA) is realized. Then, the Integrated Detector Dewar Cryocooler Assembly (IDDCA) is presented. The last part is dedicated to the electro-optical performances of the focal plane array.

2. DETECTOR ARRAY

The first key aspect in the development of high performance FPA IR detector is the ability to grow high quality HgCdTe material on a perfectly matched lattice and high quality substrate.

Large mono-crystalline CdZnTe substrates (Φ = 90mm) are routinely grown in LYNRED. These substrates are (111) oriented to allow HgCdTe growth. Zn ratio is precisely controlled in the range 1% to 5% to ensure a lattice match with the HgCdTe layer. Temperature profiles and Cd pressure control lead to high quality material with typical dislocations density in the 1.10^4 cm^{-2} range. No micro-defects larger than 1µm, such as precipitates, are observed [4].

HgCdTe is subsequently grown on CdZnTe by liquid phase epitaxy. HgCdTe crystalline quality is as high or better than that of the substrate. A very low residual doping for HgCdTe is obtained below $1.10^{15}cm^{-3}$. Flatness of the epitaxial layer has been optimized to ensure a high yield of flip-chip hybridization. eSWIR cut-off wavelength is 2.5µm at 190K.

The HgCdTe diode array process is carried out with Lynred legacy n on p planar technology based on Hg vacancies doped material in the absorbing layer. p-type doping level is fixed in the $1.10^{16}cm^{-3}$ range to reduce the dark current and maximize the operating temperature. One of the main advantages of the planar technology, used for this prototype, is the ability to passivate the HgCdTe surface without any defects. A sketch of the planar HgCdTe technology is presented in Figure 1.

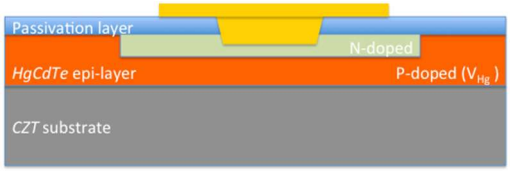

Figure 1 : Sketch of the planar n on p HgCdTe technology

The n-type doped region is achieved by ion implantation in HgCdTe. Dimensions of the implantation are critical for the design of the junction and the performances of the FPA. Finally, contact metallization is made on diodes and in the p-doped contact layer.

3. READ-OUT INTEGRATED CIRCUIT

In the frame of this development, the Read-Out Integrated Circuit (ROIC) is well known for a different use-case. It is usually operating at 110K and with a 100Hz frame rate. For this specific eSWIR application, the targeted operating temperature is 190K and the expected frame rate is in between 150 and 300Hz.

This ROIC integrates a Capacitive Trans-Impedance Amplifier (CTIA) architecture input stage at the pixel level. The objective of such stage is to improve sensitivity, linearity and noise.

The native image resolution is 640x512, with a 15µm pitch. The ROIC analog outputs reach a maximum pixel frequency of 15MHz. Therefore, in order to reach a frame rate as high as 200Hz, the ROIC has to be windowed in a 512x512 format. To reach over 300Hz frame rate, the ROIC can for instance be windowed down to a 640x256 format. This kind of format is useful for in-line control. At full frame resolution, a 150Hz frame rate is achievable. The main characteristics of the ROIC are presented in Table 1.

Table 1: Main characteristics of the eSWIR high speed ROIC.

	eSWIR high-speed ROIC
Format	640x512
Pitch	15µm
Input stage	CTIA
Readout mode	ITR, IWR
Operating temperature	190K
Storable charge	0.96Me-
ROIC Noise	200e-
Linearity	+/-1%
Frame rate	200Hz (512x512 format) 300Hz (640x256 format)
Consumption	140mW
Functions	Windowing Line/row inversion

The ROIC noise is dominated by the noise at the output of the pixel. It increases as the square root of the temperature. Consequently, it increases at 190K compared to 110K to a value of 200 electrons. The consumption of the ROIC is mainly associated to the

CTIA, which is independent of the temperature.

4. FOCAL PLANE ARRAY PROCESSING

Lynred masters flip-chip hybridization of VGA format with 15µm pitch. For 20 years, an important work has been done to optimize the CMOS ROIC preparation and hybridization itself. Hybridization is performed using Indium bumps with a flip-chip equipment. This hybridization has excellent process yield and reliability at cryogenic operating temperature. The substrate is then thinned and an anti-reflecting coating is deposited on the incident side of the FPA. Figure 2 presents one eSWIR FPA.

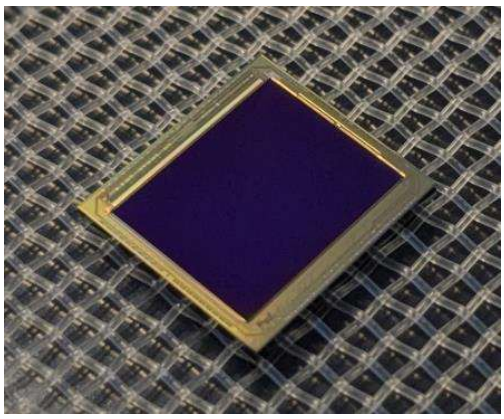

Figure 2: Picture of eSWIR high speed FPA.

5. ELECTRO-OPTICAL PERFORMANCES

A number of advanced characterizations have been realized on these FPAs. First, on different FPAs, dark current have been evaluated. Figure 3 presents the dark current as a function of 1000 over the temperature.

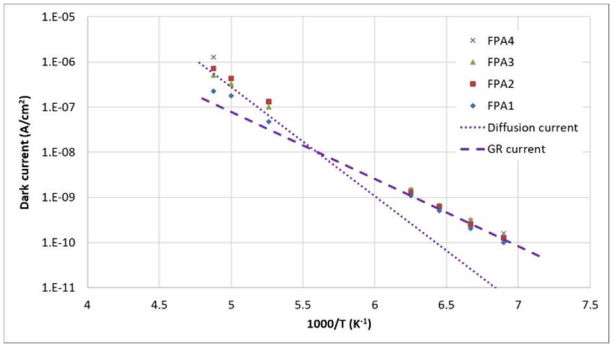

Figure 3: Dark current as a function of 1000/T for 4 different FPAs.

According to Figure 3, the dark current is reproducible between the different FPAs. Two sets of data are acquired at the operating temperature (190K – 210K) and a low temperature (145K – 160K). Dark current is in the range of 10-7A/cm2 at the operating temperature of 190K. Dark current simulations have been performed to identify the different regimes of the latter. It is in the diffusion regime with an activation energy close to the band gap at high temperature. In this regime, the dark current is ruled by the characteristics of the absorbing layer, doping level, lifetime and thickness. On the other hand, at low temperature, the dark current follows a EG/2 behavior. It points out in this regime dark current is ruled by the defects in the space charge region.

Then, the quantum efficiency has been characterized as a function of the wavelength. It is represented in Figure 4.

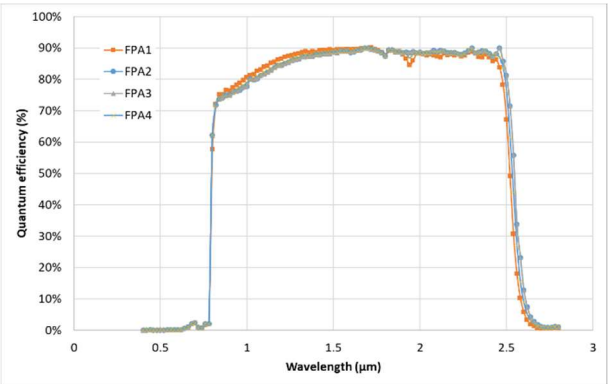

Figure 4: Quantum efficiency as a function of the wavelength.

According to Figure 4, the cut-off wavelength is in the range from 2.52 to 2.55µm. The mean Quantum Efficiency (QE) integrated in the range from 0.8 to 2.5µm is higher than 80%. This value points out a 100% fill factor of the pixel and an efficient collection of the minority carriers.

The last figure of merit in this set of advanced characterizations is the modulation transfer function as a function of the spatial frequency. The Modulation Transfer Function (MTF) is an important figure of merit as it accounts for the detector range. The MTF has been evaluated thanks to a knife-edge setup.

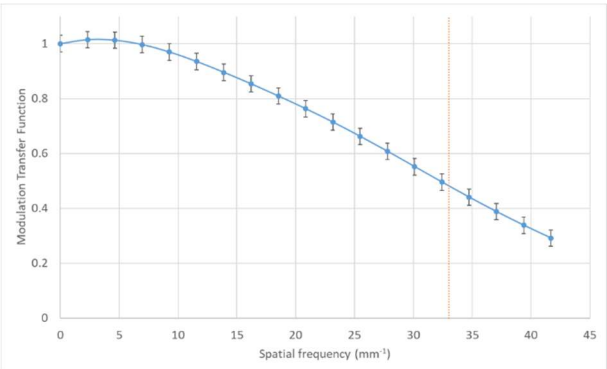

Figure 5: Modulation Transfer Function as a function of the spatial frequency.

The value reported is the mean value over a large number of pixels of the FPA. A figure of merit to illustrate the MTF performance is the value at the Nyquist frequency which is highlighted thanks to the vertical dotted lines. According to Figure 5, the MTF is in the range of 0.5 at the Nyquist Frequency

(33mm-1).

In order to assess the homogeneity and the quality of the FPAs, the DC level in front a homogeneous flux is provided in Figure 6(a). The cartography is smooth and homogeneous in a VGA format 15µm pitch. The associated histogram of the DC level is presented in Figure 6 (b). According to the latter, the number of defective pixels with a +/- 20% out of the mean value is only 67 pixels.

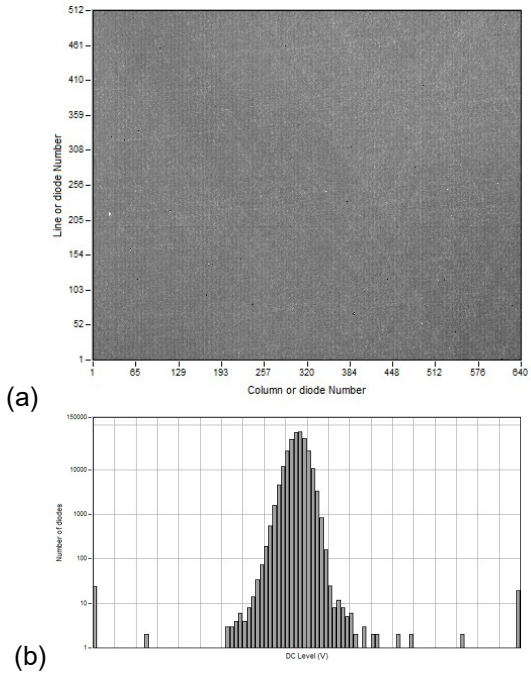

(a)

(b)

Figure 6: (a) DC level cartography, (b) histogram in front a homogeneous integrating sphere.

A second figure of merit used to characterize these FPAs in the temporal noise. Figure 7 represents the temporal noise of a FPA in front an homogeneous integrating sphere.

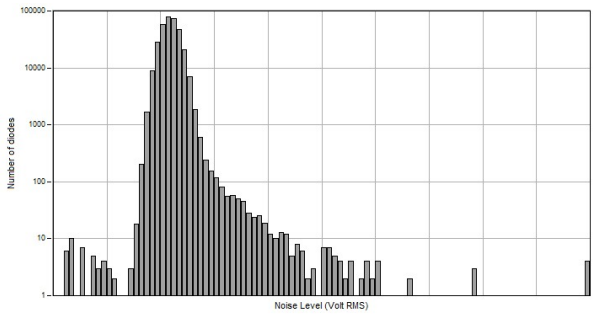

Figure 7: Histogram of temporal noise of a FPA in front a homogeneous integrating sphere.

On Figure 7, the temporal noise presents a Gaussian behavior with a limited tail in the distribution. The number of defective pixel with a +100% criteria over the mean value for defective pixels is 85 pixels.

To illustrate our manufacturing capabilities, the operability with a +100% criteria over the mean value for defective pixels is represented in Figure 8. According to the latter, the operability of the FPAs is over 99.94% of operability and reaches an operability as high as 99.97%.

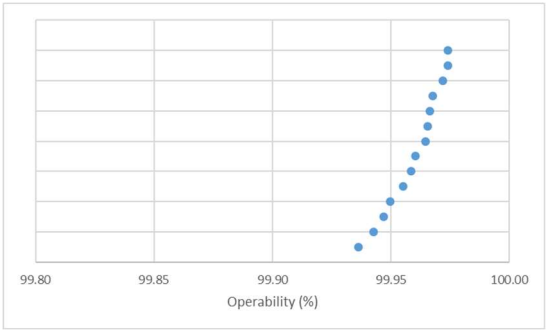

Figure 8: Cumulated operability of eSWIR FPAs with a +100% criteria over the mean value for defective pixels.

6. PRODUCT DESIGN

Lynred can deliver the Focal Plane Array to its customer. On the other hand, for customers who want to subcontract the integration in a dewar, Lynred is developing a custom Integrated Detector Dewar Cryocooler Assembly (IDDCA). The FPA are integrated into a dewar with a cryocooler. The latter is able to operate at 190K with a low consumption, below 2W as a regulated power at 20°C. A preliminary drawing of the IDDCA is presented in Figure 9. This detector allows the easy integration of a customer-specific C-Mount optics. The detector also comes with integrated proximity electronics broad.

(a)

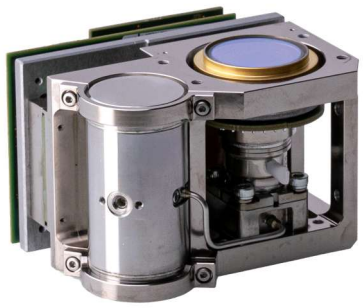

(b)

Figure 9: (a) Schematic of the Integrated Detector Dewar Cryocooler Assembly integrating the eSWIR FPA, its electronic board and equipped with a C-mount customer-

specific optics. (b) Front side picture of the IDDCA.

No cold filter is introduced on the optical path of the IDDCA. Parasitic flux is minimized thanks to a cold shield. On top of the IDDCA, a specific window with a high transmission in the range 0.8 - 2.5µm is introduced. The design of the IDDCA is leading to the best transmission of the incident flux to maximize the signal to noise ratio.

This first demonstrator is already acquiring data in the Lynred's Application Lab. The first picture was a photography of a part of the project team; see Figure 10.

Figure 10: Picture of a part of the project team.

7. CONCLUSION

In this paper, a full description of a high-speed eSWIR FPA is realized. This FPA can be delivered to customers. The operating temperature is 190K. A frame rate of 300Hz can be reached with a 640x256 format. At full frame resolution (640x512), a 150Hz frame rate is achievable. At the operating temperature, the dark current is evaluated to 10-7A/cm2 with an integrated Quantum Efficiency over 80% in the wavelength range from 0.8 to 2.5µm. The MTF of the FPA has been measured and it is equal to 0.5 at the Nyquist frequency. FPAs have been presented with an operability over 99.9%. This FPA can be integrated in a custom IDDCA. The Lynred's Application Lab is already acquiring data with this demonstrator.

8. ACKNOWLEDGEMENTS

The authors would like to thank all the Lynred's teams dedicated to a quality work to the high-speed eSWIR imager.

9. REFERENCES

1. Kou, L., Labrie, D., Chylek, P., "Refractive indices of water and ice in the 0.65- to 2.5-µm spectral range," Appl. Opt. 32, 3531-3540 (1993).

2. Tennant, W., Lee, D., Zandian, M., Piquette, E., Carmody, M., "MBE HgCdTe Technology: A Very General Solution to IR Detection, Described by "Rule 07", a Very Convenient Heuristic," J. Electron. Mater. 37, 1406–1410 (2008).

3. Bouakka-Manesse, A., Jamin, N., Delannoy, A., Fièque, B., Leroy, C., Pidancier, P., Vial, L., Chorier, P., Péré Laperne, N., "Space activity and programs at Sofradir," Proceedings Volume 10000, Sensors, Systems, and Next-Generation Satellites XX; 100000N (2016).

4. Castelein, P., Baier, N., Gravrand, O., Mollard, L., Brellier, D., Rochette, F., Kerlain, A., Rubaldo, L., Reibel, Y., and Destéfanis, G., "Latest developments on p-on-n HgCdTe architectures at DEFIR," Proc. of SPIE 9070, 90702Y-1 (2014).